AAAS
Journal of Remote Sensing
Article ID 9868564

Research Article

Continued Increases of Gross Primary Production in Urban Areas during 2000–2016

Yaoping Cui,[1,2] Xiangming Xiao,[3] Jinwei Dong,[4] Yao Zhang,[3] Yuanwei Qin,[3] Russell B. Doughty,[5] Xiaocui Wu,[6] Xiaoyan Liu,[1,2] Joanna Joiner,[7] and Berrien Moore III[5]

[1]*Key Laboratory of Geospatial Technology for the Middle and Lower Yellow River Regions (Henan University), Ministry of Education, Kaifeng 475001, China*
[2]*School of Geography And Environmental Science, Henan University, Kaifeng 475004, China*
[3]*Department of Microbiology and Plant Biology, Center for Earth Observation and Modeling, University of Oklahoma, Norman, OK, USA*
[4]*Institute of Geographical Sciences and Resources, Chinese Academy of Sciences, Beijing 100101, China*
[5]*College of Atmospheric and Geographic Sciences, University of Oklahoma, OK 73019, USA*
[6]*Agroecosystem Sustainability Center, Institute for Sustainability, Energy, And Environment, University of Illinois Urbana-Champaign, Urbana, IL 61801, USA*
[7]*NASA Goddard Space Flight Center, Greenbelt, MD 20771, USA*

Correspondence should be addressed to Xiangming Xiao; xiangming.xiao@ou.edu

Received 31 October 2021; Accepted 25 July 2022

Urbanization affects vegetation within city administrative boundary and nearby rural areas. Gross primary production (GPP) of vegetation in global urban areas is one of important metrics for assessing the impacts of urbanization on terrestrial ecosystems. To date, very limited data and information on the spatial-temporal dynamics of GPP in the global urban areas are available. In this study, we reported the spatial distribution and temporal dynamics of annual GPP during 2000–2016 from 8,182 gridcells (0.5° by 0.5° latitude and longitude) that have various proportion of urban areas. Approximately 79.3% of these urban gridcells had increasing trends of annual GPP during 2000-2016. As urban area proportion (%) within individual urban gridcells increased, the means of annual GPP trends also increased. Our results suggested that for those urban gridcells, the negative effect of urban expansion (often measured by impervious surfaces) on GPP was to large degree compensated by increased vegetation within the gridcells, mostly driven by urban management and local climate and environment. Our findings on the continued increases of annual GPP in most of urban gridcells shed new insight on the importance of urban areas on terrestrial carbon cycle and the potential of urban management and local climate and environment on improving vegetation in urban areas.

1. Introduction

Urbanization is a process with large changes in demography and land transformation and management [1, 2]. Global urban area was 0.65 million km^2 in 2000 and could increase to 1.2 million km^2 by 2030 [3]. At present, more than 50% of the global population (7+ billion) live in urban areas, and approximately 70%–90% of economic activities take place there [4, 5]. Urban areas, including both urban sprawl and urban footprint, where there is close nature and human connections (cities, suburban, periurban, and neighboring rural areas), tend to experience more intensive and complex changes of local climate and environment than do the remote rural areas [6–10]. As urban ecosystems are complex and dynamic, it has been a challenge to quantify and understand urban ecosystem structure, function, and service [11, 12].

First, urbanization is characterized by an expansion of impervious surfaces (e.g., roads, houses, and buildings) within city administrative boundary. During urban expansion, croplands and other natural landscapes were converted to impervious surface [10, 13]. A few studies investigated the impacts of urban impervious surface (UIS) expansion on vegetation production and the carbon cycle in the urban areas, and they reported losses of vegetation production

and terrestrial carbon storage, primarily driven by the expansion of urban impervious surface into vegetated areas [10, 14, 15]. Second, urbanization is characterized by urban land management, which affects the change and expansion of vegetation within the city administrative boundary and nearby rural areas. As urban economy developed over time, many cities increased their vegetation coverage and developed multilayer vegetation structure. Third, urbanization is characterized by the changes of local climate and atmospheric composition in urban, suburban, periurban, and neighboring rural areas [16, 17]. A few studies investigated the effects of land cover change and local climate on vegetation in the large cities and reported increased tree productivity and vegetation greenness in many cities [18, 19]. Zhong et al. investigated the spatial-temporal dynamics of urban expansion, vegetation greenness, and GPP in megacity Shanghai, China, during 2000-2016 [20], and Cui et al. analyzed the interannual changes of GPP over the ten most populous megacities in the world during 2007-2014 [21]. These two studies reported that there were large spatial-temporal changes of GPP and GPP increased over years in these megacities.

Many studies have investigated the spatial-temporal changes of global GPP [8, 22, 23], but the impacts of urbanization on GPP at the global scale have received little attention and are not well understood. The first reason is that the urban areas account for a small proportion of the global landmass. The second reason is that there are many types of land cover types within a city, and thus it is very difficult to model and estimate GPP for those pixels that are classified as urban. In several global GPP datasets, the pixels that are classified as urban have GPP value of zero or no data, for example, the MODIS GPP/NPP data product (MOD17) [24]. The third reason is that it is very hard to define the urban areas as the city administrative boundary changed its sizes and shapes frequently over years. Several studies reported the effect of urbanization on vegetation could reach beyond the city administrative boundaries [7, 25, 26]. To address these issues, many studies have used gridcell-based data at various spatial resolutions (e.g., 500 m, 5 km, and 0.5°) to study urban ecosystems [20, 21, 27, 28].

A gridcell at coarse spatial resolutions (e.g., 5 km or 0.5°) could cover (1) city area only, (2) rural area only, and (3) a mix of both city and rural areas. Theoretically, urban expansion within a gridcell started with an increase in urban impervious surface (UIS), which reduce urban-rural vegetation (URV) [21]. Urban land management also affects URV, including (i) land cover change (such as new lawns, open parks, and green-belts); (ii) vegetation species change and growth in suburban, periurban, and neighboring rural areas; and (iii) vegetation management (such as fertilization and irrigation) [29, 30]. In recent years, many cities started to improve and expand urban vegetation and considered urban vegetation as one of major metrics for the society to address the ecological and environmental impacts of urbanization [31]. A few studies reported increased vegetation greenness and lengthened growing seasons in urban areas over Mexico City and the U.S. Great Plains [29, 32]. Other studies found enhanced vegetation growth in urban areas, driven by elevated temperature and atmospheric CO_2 concentration and favorable light and wind conditions [33–35], and the changes of urban plant species in urban areas [36, 37].

In this study, we investigated the spatial-temporal changes of GPP in the urban areas over the globe, which serves as an indicator for us to assess the effects of (1) urban expansion (UE, as measured by UIS) and (2) urban management and climate (UMC) on vegetation (URV). We analyzed annual GPP data from the satellite-based Vegetation Photosynthesis Model (VPM) [38, 39] and quantified the effects of urbanization on GPP in urban areas over the world. The global urban extent data and GPP data during 2000–2016 were used and organized into 0.5° (latitude and longitude, ~50 km at equator) spatial resolution, and most of the resultant gridcells have cities, suburban, periurban, and neighboring rural areas. This study will identify those gridcells that had losses or gains or no substantial changes of GPP as urban expansion continued over the years, which would shed new insights on the effects of urbanization on GPP in urban areas (or urban ecosystems).

2. Materials and Methods

2.1. Global Urban Area Expansion Data. We used the global urban area expansion dataset that was developed by the Seto Laboratory at Yale University. The original raster dataset has a spatial resolution of 5 km, and the urban area estimates for 2030 was generated by overlaying 1,000 forecasts of urban expansion [3]. In the raster dataset, the category 101 represents existing urban area gridcells in 2000, and the categories from 0 to 100 refer to gridcells that may become urban area by 2030 with a probability ranging 0 to 100. Following the same definition and procedure described in the Seto's study [3], we used 75% as a threshold to define the urban area gridcells in 2030 as 75%–100% range basically represents a "most likely occur" case. The number of gridcells with a probability of >75% accounts for more than 85% of the total number of gridcells with a probability of >50%. The urban area data in 2000 and 2030 at 5-km spatial resolution was aggregated to $0.5° \times 0.5°$ (-135.8°W~177.8°E and -54.75°S~65.25°N) gridcells, and then we calculated percentage (%) of urban areas within individual gridcells. We selected those gridcells that contain more than 1% urban area in 2000 to represent urban-related gridcells [5, 40]. We calculated the difference between urban area in 2000 and projected urban area in 2030 and then did linear interpolation to estimate urban area in 2016 (Figure S1). Note that one global dataset of impervious surface from analyses of satellite images has recently been produced and could be used in future study [41, 42]. We compared the impervious surface data from this study (the years of 2000 and 2016) with the impervious surface data from the GLC_FCS30 (the years of 2000 and 2015) at a spatial resolution of $0.5° \times 0.5°$ [42]. The fitting coefficients (R^2) between these two datasets were 0.67 in 2000 and 0.62 in 2016, respectively ($P < 0.05$), which shows a reasonable consistency between these two impervious surface datasets in 2000 (Figure S2). The bias in impervious surface area estimates between these two datasets in 2015(2016) could be attributed to the fact that the GLC data in 2015 were derived from analyses of satellite images. In this study, we used

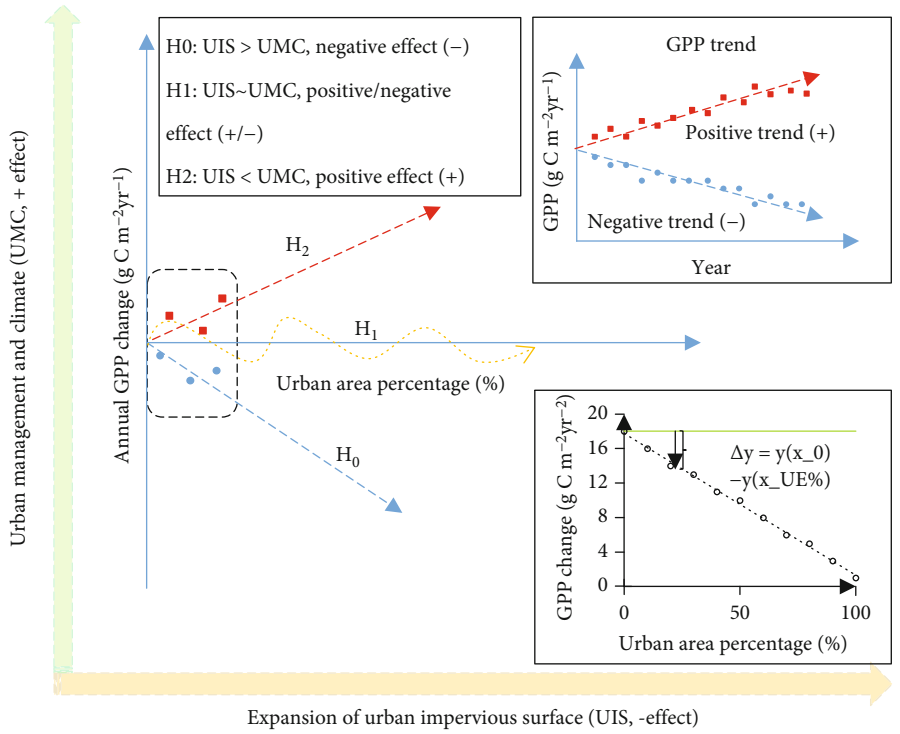

Figure 1: The hypothesis and analysis framework in this study. Vegetation within an urban gridcell (URV or GPP) is affected by (1) expansion of urban impervious surface (UIS), which is a metric for urban expansion (UE), and (2) urban management and climate (UMC). Annual GPP trend ($g\,C\,m^{-2}\,yr^{-1}$) means the interannual GPP variation over year. H_0, H_1, and H_2 (red, yellow, and blue lines) are three-basic hypothesis for analyzing offsetting effects of urbanization on GPP. To further quantify the impact of urbanization on annual GPP (ΔGPP), we hypothesize that there is a linear relationship between the changes in percent urban areas (ΔUIS) and the annual GPP trends. The subfigure in upper left and lower right corners are the explanatory charts to calculate the GPP loss caused by the negative impact of UIS ($\Delta y = \Delta$GPP).

"urban gridcells" at 0.5° spatial resolution as our study areas (20.5 million km^2) for two reasons. First, urban gridcells at such coarse spatial resolution could cover urban, suburban, periurban, and any adjacent rural areas which may have a certain degree of socioeconomic and functional integration with urban areas [3, 7]. Second, we used the GOME-2 solar-induced chlorophyll fluorescence (SIF) data at 0.5° spatial resolution to evaluate urban GPP data (see Section 2.2).

2.2. Global Gross Primary Production (GPP) Data. Global GPP dataset at 500-m spatial resolution and 8-day temporal resolution during 2000–2016 was from the satellite-based Vegetation Photosynthesis Model (VPM) [38, 39]. In order to be consistent with the spatial resolution of urban area dataset and the GOME-2 SIF dataset, GPP data were spatially aggregated to a $0.5° \times 0.5°$ grid. We generated the monthly and annual GPP data by summing the initial 8-day GPP data.

2.3. GOME-2 Solar-Induced Chlorophyll Fluorescence Data. Solar-induced chlorophyll fluorescence (SIF) is the energy emitted by plants after chlorophyll absorbs photosynthetically active radiation (PAR). We obtained the SIF data from the Global Ozone Monitoring Instrument 2 (GOME-2), and the SIF (V26) dataset during 2007-2016 has a spatial resolution of $0.5° \times 0.5°$ grid and monthly temporal resolution [43]. As SIF is related to light absorption by green vegetation, many studies reported strong linear correlation between SIF and GPP over weekly to monthly time scales [21, 43–45]. In a previous study, we also evaluated the consistency in seasonal dynamics of GPP and GOME-2 SIF in ten megacities [21]. In this study, we analyzed the spatial-temporal consistency between SIF and GPP over all the urban gridcells in the world.

2.4. Analytic Framework on the Effect of Urbanization on GPP. To quantify the impact of urbanization on GPP over years within individual urban gridcells, we developed a conceptual framework that considers the effects of both urban expansion (as measured by UIS) and urban management and climate (UMC) on urban-rural vegetation (URV) and frames the hypotheses on their likely impacts on GPP dynamics, based on literature review and synthesis. Urbanization could have positive and negative impacts on URV, and we use GPP as the metric for URV in this study. First, urban expansion (expansion of impervious surface) in the urban gridcell (UIS) could result in a loss of vegetation (URV) that is a negative effect (-) on GPP. Improved urban management and local climate within the urban gridcell (UMC) could have a positive effect (+) on URV and GPP (Figure 1). We propose three hypotheses on the impacts of urbanization on interannual trends of annual GPP: (i) H_0: The impact of UIS on GPP is similar to the impact of UMC on GPP, which results in no net change in annual GPP; (ii) H_1: The impact of UIS on GPP is larger than the impact of UMC on GPP, which results in a decrease of annual GPP; and (iii) H_2: The impact of UIS on

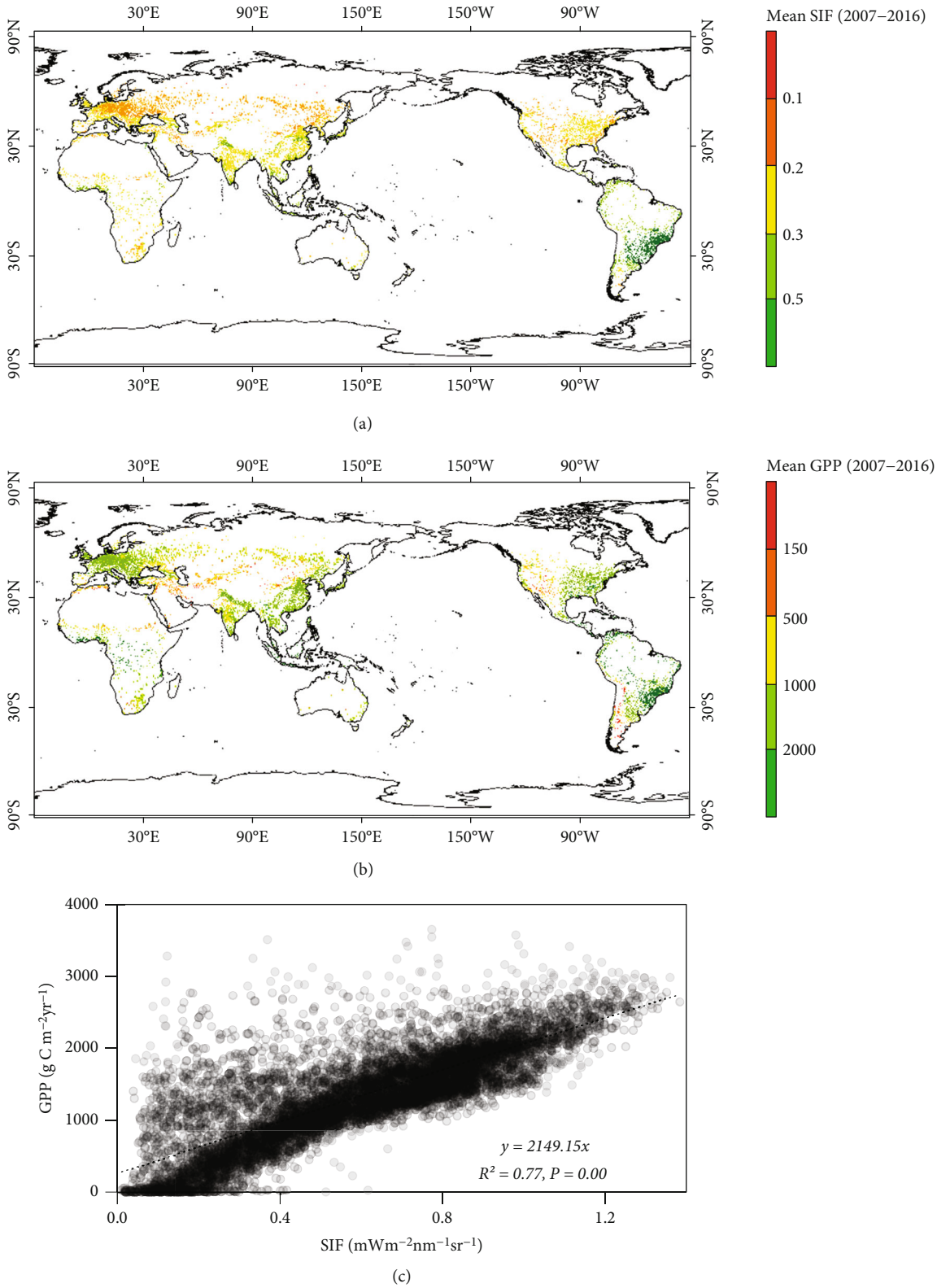

1 Figure 2: Spatial distributions of multiyear mean SIF and GPP during 2007-2016 in all the urban gridcells. (a) SIF data; (b) GPP data; (c) the scatterplot between GPP and SIF for individual urban gridcells.

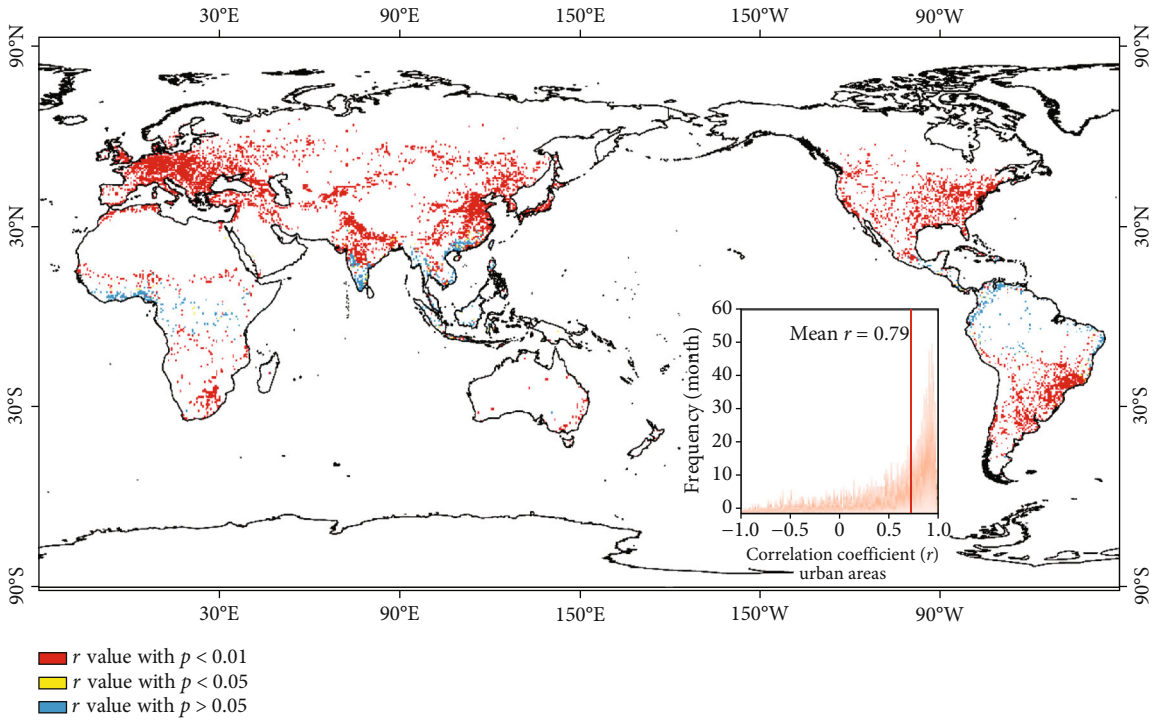

Figure 3: spatial distribution of the correlation coefficient (R) between monthly SIF and GPP during 2007-2016.

GPP is smaller than the impact of UMC on GPP, which results in an increase of annual GPP.

In the conceptual framework, we hypothesize that there is a linear relationship between the changes in percent urban areas within urban gridcells and the changes of GPP over years. Then, a linear equation can be used to express the negative impact of UIS on GPP trend:

$$\mathrm{mGPP} = \beta \times \Delta\mathrm{UIS} + \alpha, \quad (1)$$

which shows the linear relationship between ΔUIS and the GPP interannual trend; the unit of mGPP is $\mathrm{g\,C\,m^{-2}\,yr^{-1}\%^{-1}}$; the unit of ΔUIS is percent of the urban area (%); α and β are the fitting parameters. As shown in Figure 1, the parameter β can be negative and hypothesis for analyzing effect of urbanization on GPP is H_1.

The annual GPP trend before urbanization or without the impact of urbanization is equal to α (ΔUIS = 0); the unit of α is $\mathrm{g\,C\,m^{-2}\,yr^{-1}}$. Then, the loss of annual GPP trend caused by expansion of impervious surface (ΔGPP) can be calculated as

$$\Delta\mathrm{GPP} = \alpha - \mathrm{mGPP} = \alpha - (\beta \times \Delta\mathrm{UIS} + \alpha) = -\beta \times \Delta\mathrm{UIS}. \quad (2)$$

Finally, the GPP interannual loss (LGPP) along with the increasing of percent urban areas (ΔUIS) can be reconstructed using

$$\mathrm{LGPP} = \Delta\mathrm{GPP} \times \mathrm{Year}, \quad (3)$$

$$\mathrm{SGPP} = \mathrm{sum}\,(\mathrm{LGPP} \times \mathrm{Area}), \quad (4)$$

where the unit of LGPP is $\mathrm{g\,C\,m^{-2}}$. SGPP is the global total GPP loss caused by UIS; and its unit is g C.

3. Results

3.1. Spatial-Temporal Consistency between GPP and SIF in Urban Areas. As shown in Figures 2(a) and 2(b), there is good agreement in the spatial distributions of multiyear mean SIF and GPP during 2007-2016 over the 8,182 urban gridcells. High SIF and GPP values mainly occurred in the Southeastern Brazil and Argentina. Multiyear mean SIF and GPP were $0.68\,\mathrm{mW\,m^{-2}\,nm^{-1}\,sr^{-1}}$ and $966.16\,\mathrm{g\,C\,m^{-2}\,yr^{-1}}$, respectively. The maximum SIF and GPP during 2007-2016 were $1.4\,\mathrm{mW\,m^{-2}\,nm^{-1}\,sr^{-1}}$ and $3910.61\,\mathrm{g\,C\,m^{-2}\,yr^{-1}}$, respectively. A 2-dimensional scatterplot of SIF versus GPP shows significant correlation between SIF and GPP in the urban gridcells (Figure 2(c)).

Most of the gridcells and urban gridcells showed the significant linear correlation between monthly SIF and GPP, especially in urban gridcells in the middle to high latitudes (Figure S3). The annual and monthly mean SIF and GPP from 2007 to 2016 also showed good temporal consistency. Furthermore, the correlation analysis indicates that 78% of urban gridcells pass the significant test of 0.05. Annual GPP and SIF show a strong linear relationship (correlation coefficient $r = 0.79$), providing additional confidence in our GPP data that are used for the study of urban areas (Figure 3).

3.2. Magnitude and Interannual Trends of GPP in Urban Areas. Of the total 58,158 half-degree land gridcells (excluding Antarctica and Greenland) over the globe, 8,182 gridcells had a range of 1% to 69% urban areas in 2000 (Figure 4(a)), with a mean value of 3.3% and standard deviation of 4.8% (Figure 4(a) and

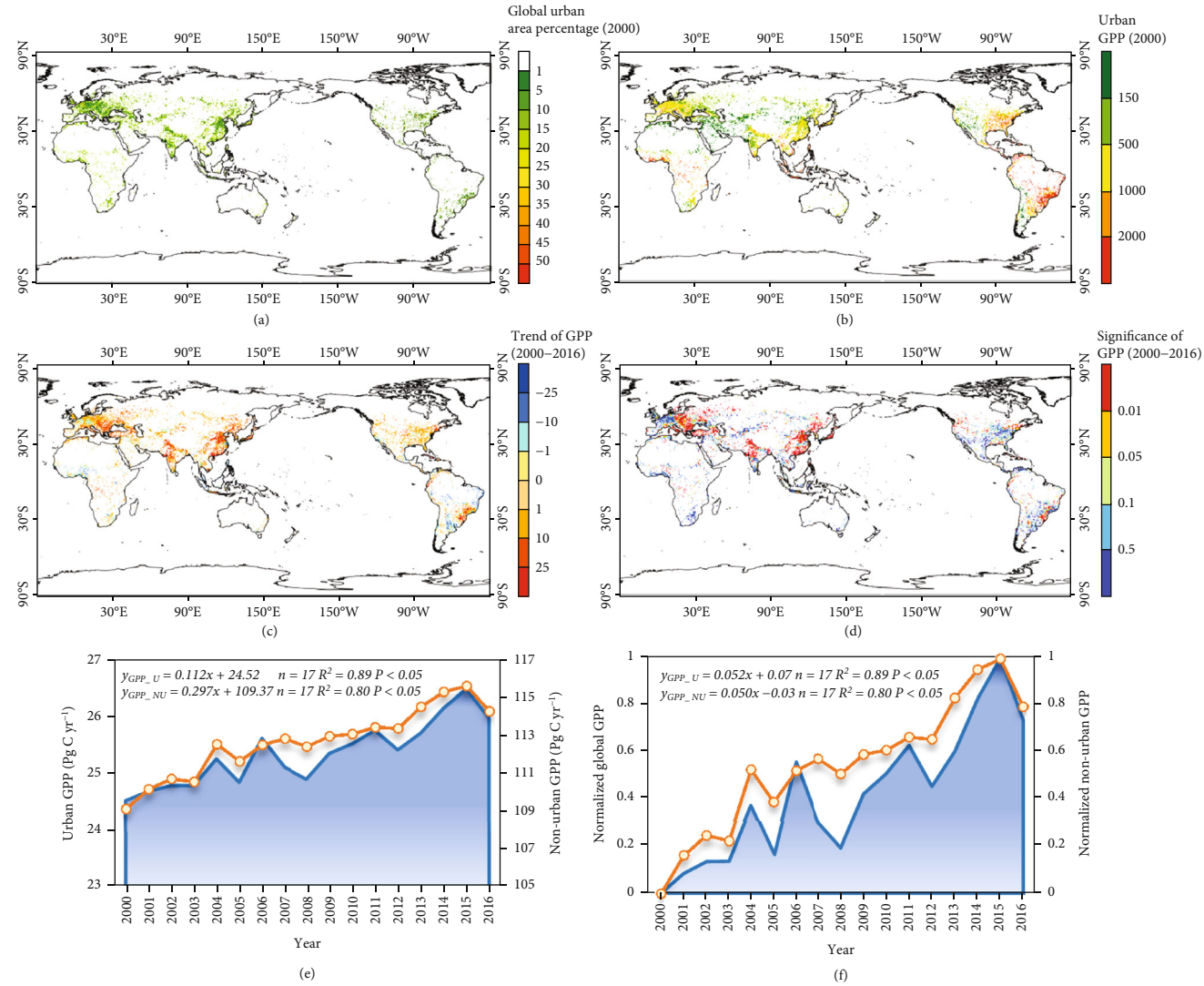

Figure 4: Spatiotemporal variations of urban GPP and nonurban GPP in the world. (a) Spatial distribution of urban gridcells; (b) mean annual GPP in urban gridcells in 2000; (c) interannual trend of urban GPP during 2000–2016; (d) P value significance test for the interannual trend of urban GPP during 2000–2016; (e) interannual variation of urban GPP (GPP_U, GPP within urban gridcells, and warm color) and nonurban GPP (GPP_NU, GPP within nonurban gridcells, and cool color); and (f) corresponding result after normalization of urban GPP and nonurban GPP by (GPP – GPPmin)/(GPPmax – GPPmin).

Figure S4). In 2000, these 8,182 urban gridcells cover a total of 20.5 million km^2 land area. The mean value of annual GPP within these urban gridcells in 2000 is 1,215.8 g C m^{-2} yr^{-1} (Figure 4(b)). Approximately, 63.1% of these urban gridcells had annual GPP of ≥1000 g C m^{-2} yr^{-1} (Figure 4(b)). In 2000, the ratio of urban GPP (GPP within urban gridcells) to global land GPP was 20.8%, which was higher than the ratio (15.4%) of urban gridcell area over global land area (132.8 million km^2, excluding the Antarctic continent and Greenland).

The annual rates of changes in urban GPP during 2000–2016 among the 8,182 urban gridcells had substantial spatial variations and range from -55.34 to 43.38 g C m^{-2} yr^{-1} (Figures 4(c) and 4(d)). A total of 6,482 gridcells had increasing trends of annual GPP during 2000–2016, with a mean value of 9.1 g C m^{-2} yr^{-1}. The remaining 1700 (20.8%) urban gridcells had decreasing trends, with a mean value of -7.11 g C m^{-2} yr^{-1}.

The total annual GPP in the 8,182 urban gridcells varied from 24.38 Pg C in 2000 to 26.1 Pg C in 2016, with an annual increasing rate of 0.11 Pg C yr^{-1} (Figure 4(e)). The total annual GPP from the nonurban gridcells varied from 109.57 Pg C in 2000 to 113.92 Pg C in 2016, with an annual increasing rate of 0.30 Pg C yr^{-1}. In order to eliminate the possible interference caused by the value size of the global and urban GPP to the interannual changes and be convenient for directly comparison, a dimensional expression is transformed into a dimensionless expression. We normalized the rates of changes for urban GPP and nonurban GPP, and the resulting annual rate of change in the GPP in urban areas was similar to that of the nonurban GPP (0.052 vs. 0.050), and the interannual variation of nonurban GPP during 2000-2016 was slightly larger than that of urban GPP (Figure 4(f)).

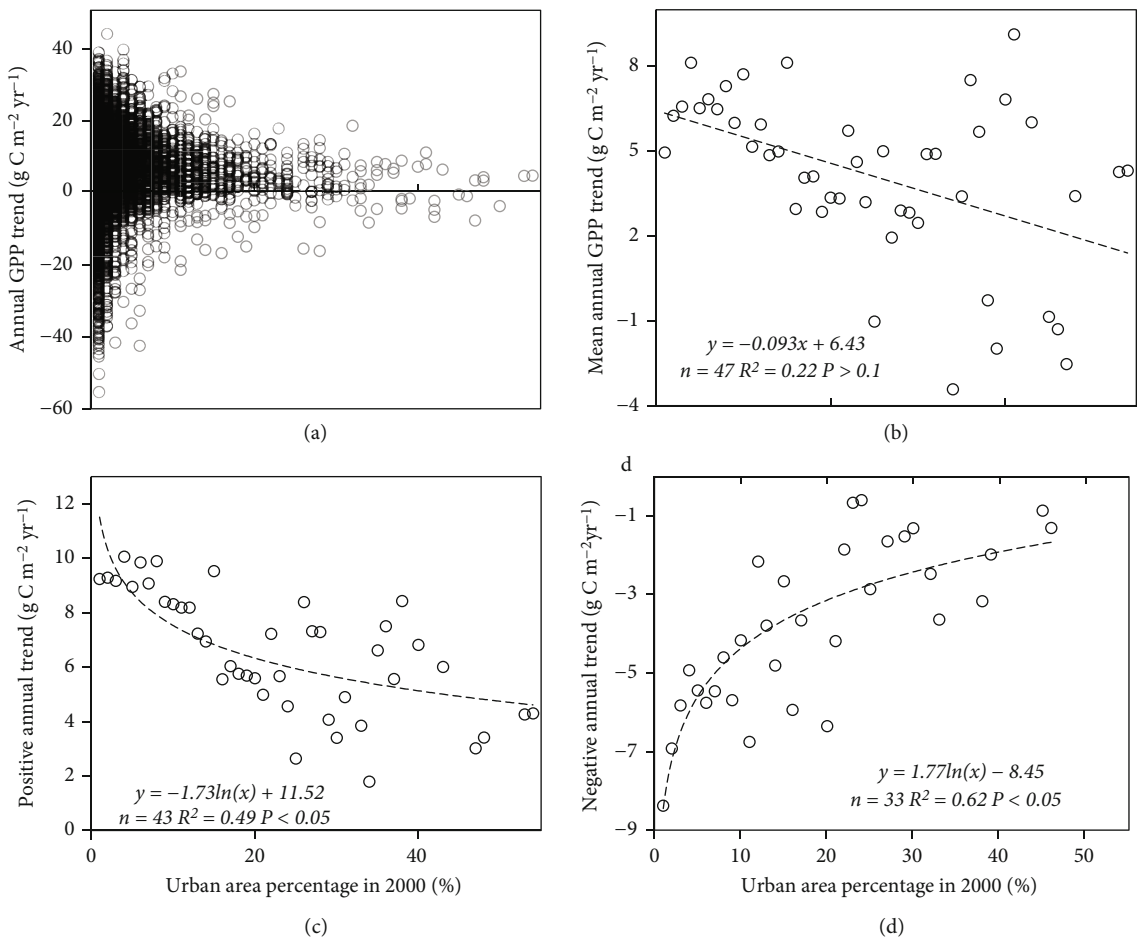

Figure 5: Relationship between annual GPP trend and percentage of urban area in 2000. (a) Scatterplot of annual GPP trend and percent urban areas for 8,182 gridcells. (b) Scatterplot of mean annual GPP trend and percent urban areas in 2000 for 8,182 gridcells. (c) Relationship between mean annual GPP trend (positive trend) and percent urban areas in 2000 for 6,488 gridcells. (d) Relationship between mean annual GPP trend (negative trend) and percent urban areas in 2000 for 1,694 gridcells. The y-axes of (b), (c), and (d) are binned, and the bin width of urban area percentage is 1%.

3.3. Effects of the Percent Urban Areas in 2000 on the Interannual Trends of GPP during 2000–2016. We investigated to what degree the interannual trends of GPP during 2000–2016 were affected by urban areas in 2000 (treated as an initial condition). Interannual trends of GPP in the urban gridcells have a dispersive distribution along percent urban areas within the urban gridcells in 2000 (Figure 5(a)). Those urban gridcells with small percentages of urban area in 2000 have larger variations of GPP trends among the gridcells, in comparison to those urban gridcells with a large percentage of urban area in 2000.

We calculated the averages of GPP trends by the percent urban areas within urban gridcells in 2000. The simple linear regression model shows a negative relationship between the mean annual GPP trends and percent urban areas in 2000, with a slope of -0.093 g C m^{-2} yr^{-1} over one percent urban areas within urban gridcells in 2000 (Figure 5(b)). Because GPP was affected by both UIS and UMC, the slope indicated that the net effect of urbanization was negative. The total GPP loss (SGPP in equation (4)) of 0.0061 Pg C yr^{-1} caused by initial urbanization was quantified by the observation of the relationship between GPP trends and initial percent urban areas. The ratio of "GPP loss/global GPP in 2000" was 0.025%. The results suggest that the GPP within the urban gridcells have benefit from the positive effect of UMC to some extent. The results also suggest that those gridcells with large percent urban areas in 2000 had relatively smaller potential to increase carbon uptake (GPP) due to the limited vegetation areas within an urban gridcell. Correspondingly, those gridcells with small percent urban areas in 2000 had large potential to either increase or decrease carbon uptake (GPP), dependent upon how well vegetation in urban areas were managed. We further calculated mean annual GPP trends for 6,488 urban gridcells with positive annual GPP trends (Figure 5(c)) and for 1,694 urban gridcells with negative annual GPP trends (Figure 5(d)).

3.4. Effects of Urban Area Expansion during 2000–2016 on the Interannual Trends of GPP. We calculated urban area expansion between 2000 and 2016 for individual urban gridcells (Figure 6). UIS trends in 3461 urban gridcells vary from 1% to 43%, and the remaining 4721 urban gridcells had UIS trends of less than 1% (Figure S5). Most of those gridcells with large UIS trends occurred in developing countries such as China and India.

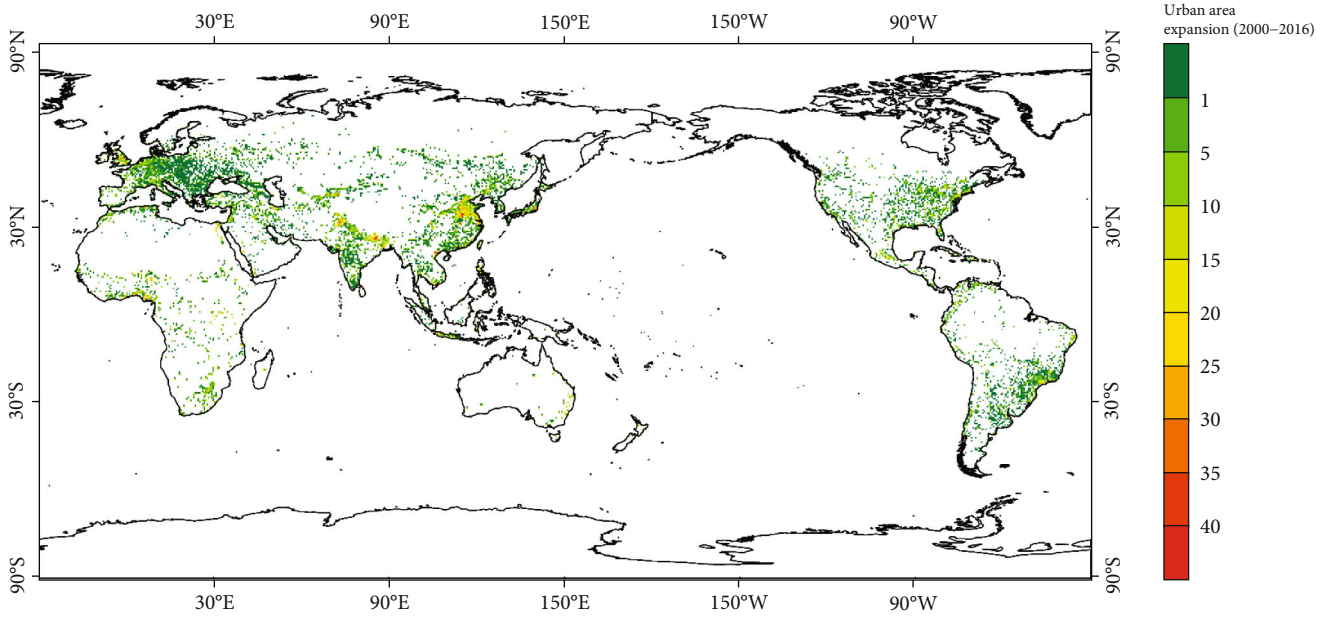

Figure 6: Urban expansion (%) within in urban gridcells from 2000 to 2016.

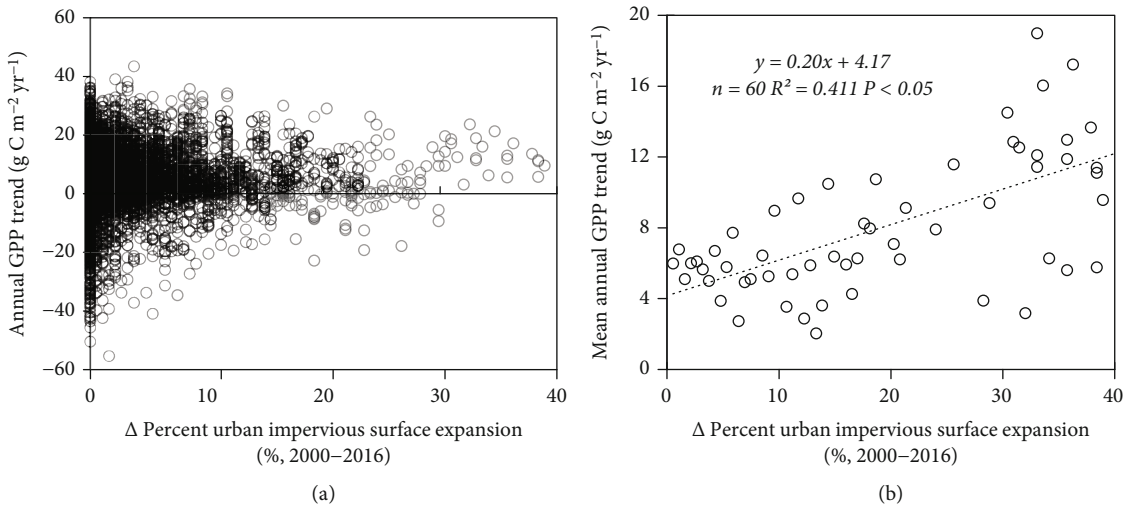

Figure 7: Relationship between interannual GPP trend and Δ% urban impervious surface expansion (UIS) from 2000 to 2016. (a) Scatterplot of GPP trend and Δ% UIS in the 8,182 urban gridcells. (b) Scatterplot of Δ% UIS and mean GPP trend (averaged GPP trends by an interval of 1% UIS).

We investigated the relationship between interannual GPP trend and UIS trend (% change) during 2000–2016 (Figure 7(a)). Based on conventional knowledge and hypothesis H_0 (Figure 1), GPP in the urban areas will decrease over these years owing to the negative impact of UIS. We used the mean annual GPP trend to fit a linear regression model for individual gridcells. The results showed that 20.7% of urban gridcells conformed to the hypothesis with UIS > UMC (negative effect, H_0 in Figure 1), and 79.3% of the urban gridcells were consistent with the hypothesis with UMC > UIS (positive effect, H_2 in Figure 1). Given the fact that annual GPP trends in urban gridcells also contain the impacts of large-scale environmental change such as global warming and increased atmospheric CO_2 concentration, we do not attribute the positive trends of GPP in urban areas solely to one single factor of UMC. However, GPP in urban areas did show a significant positive trend ($0.2\,g\,C\,m^{-2}\,yr^{-1}$) as the percentage of urban areas increased (every 1% expansion of impervious surface) over these years ($P < 0.05$, Figure 7(b)).

We assume that small urban expansion is not easy to find precisely at a large gridcell (0.5° latitude and longitude) and the urban mapping has a 5% scale error. We split the 8,182 urban gridcells into two groups: group #1 with no obvious UIS expansion (Δ% <5%) and group #2 with obvious UIS expansion correspondingly (Figure 8). The average values of annual GPP trend of group #1 and group #2 were

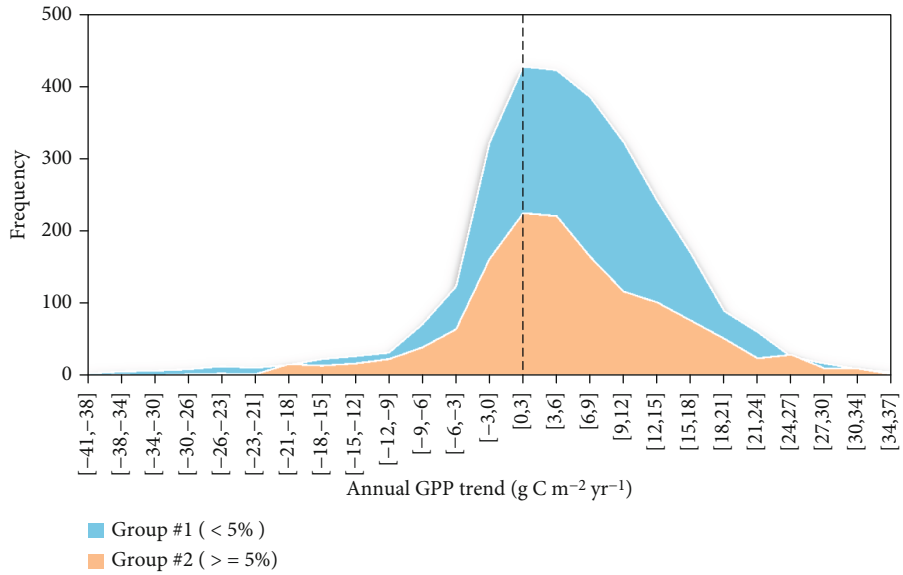

FIGURE 8: Frequency chart of annual GPP trend. Assuming that there is no urban expansion in the grid unit, and the percentage of urban expansion <5% (blue) and urban expansion ≥5% (orange), the annual GPP trend change chart.

5.54 and 5.92 g C m^{-2} yr^{-1}, respectively, showing that the change of GPP trend for the two groups were similar overall.

4. Discussion

4.1. Definition of Urban Areas and Significance of Urban GPP on Terrestrial Carbon Cycle. There are no standard definitions for urban areas [8]. Urban areas can be delineated directly by city administrative boundaries and thus include impervious surface, vegetated area, barren land, and surface water body. Impervious surface area is one of land cover types within urban areas and often used to delineate urban areas [8, 46]. The Census in America uses the population size to define urban extent [6]. Several studies reported that the effects of urbanization on vegetation are much larger than the city administrative boundaries [7, 25, 26]. In addition, urbanization could lengthen the growing season of vegetation, which increases carbon uptake by vegetation [25, 47]. In an effort to addressing these complex problems, Churkina [7, 14] proposed a concept of "urban system" and used it for their modeling study of the carbon cycle. Urban system includes both urban sprawl and urban footprint. In practice, the spatial extents of urban systems (both urban areas and their spatial impacts) are still very difficult to define and delineate, especially at the global scale. To date, there is no public dataset that delineates the administrative boundaries of all urban areas in the world and defines the spatial extents affected by urbanization. As an alternative to the urban administrative boundary dataset, it is reasonable for researchers to use urban gridcells to explore the impacts of urbanization on GPP within the urban gridcells. Many scholars have already used urban gridcells to study cities. Zhang et al. (2004) used $0.5^\circ \times 0.5^\circ$ urban gridcells to analyze the effect of urban climates on vegetation phenology [25]. Cui et al. used $0.5^\circ \times 0.5^\circ$ urban gridcells to analyze the temporal consistency between GPP and solar-induced chlorophyll fluorescence in the ten most populous megacity areas over the world [21]. In this study, we used "urban gridcells" to describe our study areas (urban areas), which can be thought of as the sum of urban, suburban, periurban, and any adjacent rural areas which may have a certain degree of socioeconomic and functional integration with urban areas (Figure 9) [3, 7].

GPP in urban areas is one of the essential components for the global carbon fluxes [7, 48, 49]. Churkina assessed the GPP from the urban areas and their footprints and reported that the total GPP amount from the urban areas varies in the range of 14–43 Pg C yr^{-1} [14]. Our results showed that the total GPP in the urban areas varied in the range of 24.38–26.1 Pg C yr^{-1}. One recent study assessed the impact of urban expansion and reported that global net primary production (NPP) had a loss of 22.4 Tg C yr^{-1} during 2000-2010, driven by urban expansion [28], while our study reported that the total GPP in urban areas increased during 2000-2016. The discrepancy between these two studies can be explained in part by the GPP/NPP datasets used in these two studies. Liu et al. 2019 study [28] used the MOD17A2 GPP/NPP datasets, which has GPP and NPP values of zero for urban pixels as the GPP/NPP model does not calculate GPP/NPP for urban pixels. In comparison, the VPM model calculates GPP for urban pixels. Figure 10 shows the spatial distributions of $GPP_{MOD17A2}$ and GPP_{VPM} over Shanghai, China. The results in Liu et al. study represent the impact of UIS expansion on vegetation GPP/NPP, a loss of GPP/NPP during 2000-2010. In comparison, the results in our study represent the impact of both UIS and UMC on vegetation GPP, a gain of GPP during 2000-2016. In addition, the sizes of urban gridcells used in these two studies also differ, which affects to some degree assessment of the effect of urbanization on vegetation over years. Therefore, careful selection of GPP datasets is needed for the study of urbanization on vegetation [28].

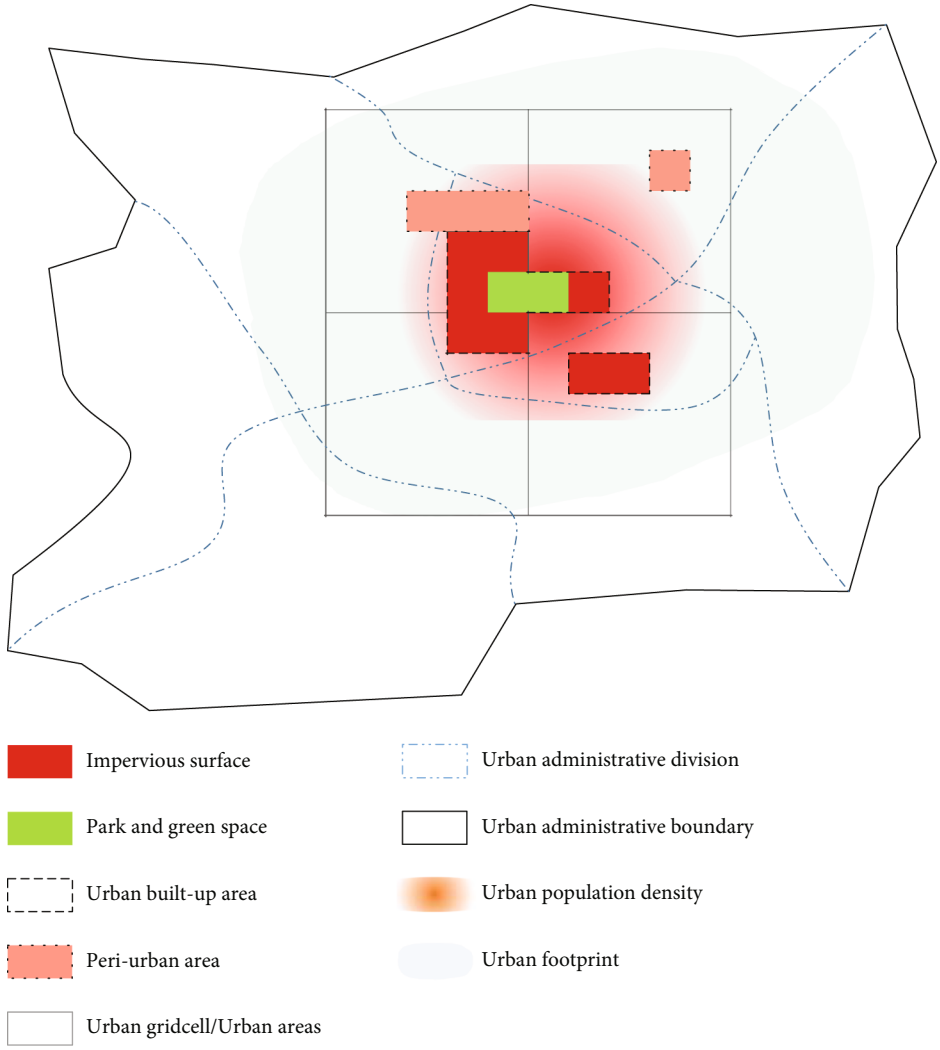

Figure 9: Urban areas and their spatial impacts.

4.2. Continued Increase of GPP in Urban Areas. It is a common view that vegetation greenness, gross, and net primary production will decrease in the process of urbanization, as urban impervious surface expansion would reduce vegetation [14, 15]. Several studies reported that the urban heat effect on vegetation phenology in and around urban areas with 0.5° and 0.25° gridcells [21, 47, 50]. In our study, benefited from the positive effect of UMC, GPP in a large proportion of the urban gridcells continued to increase during 2000–2016. For many urban gridcells, the initial urban impervious surface conditions affect GPP trend, the larger the original urban area percent is, the smaller potential of annual GPP increases. For many urban gridcells, the rates of urban expansion also affect GPP trends, the larger urban area expansion, the more increase of annual GPP. Therefore, the effect of urban expansion (or urbanization) on GPP is complex and is jointly controlled by both UIS and UMC.

The interannual variation of urban GPP was partially in conformity with that of nonurban GPP (Figure S6). Some studies have shown that NDVI and EVI of vegetation in the world and individual cities increased over the past decades [20, 23, 51]. Nonurban GPP had large drops in the years of 2005, 2008, and 2012 (Figure 4(f)), and in comparison, urban GPP had relatively small drops in those years; especially, the situation may be more pronounced in poor environmental conditions for vegetation [15] or when the GPP decreases sharply (Figure 4(f)). This actually reflects that UMC can resist the impacts of unfavorable environments on vegetation and urban areas may help reduce interannual variation of vegetation growth to a certain extent [52, 53].

The results from this study are consistent with several previous studies, which have shown evidence of both positive and negative effects of urbanization on vegetation (Table 1) [45]. In addition to urban impervious surface area expansion, people set-up new green space and plant new types of vegetation in urban areas [21, 54]. People also do effective management and protection of vegetation, including irrigation and fertilization. Furthermore, increased atmospheric CO_2 concentration and local climate also affect vegetation [55, 56]. As the results of all these varying factors, the net effects of urbanization on vegetation are location-specific, complex, and dynamics. Therefore, the study on the effects of

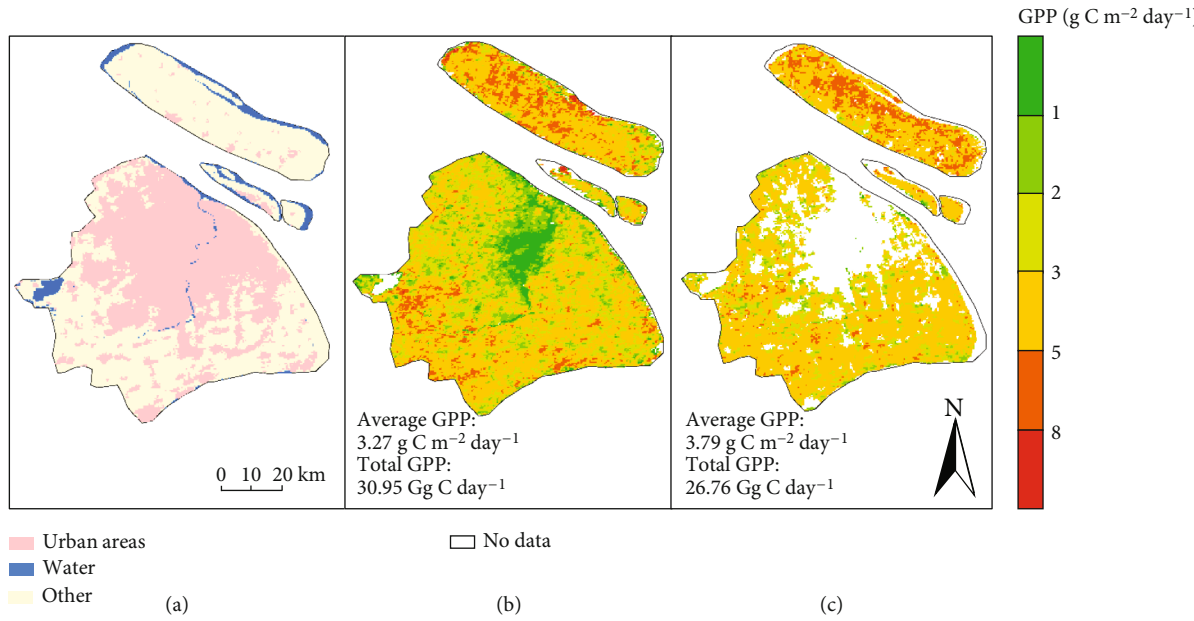

Figure 10: Spatial distributions of land cover types in 2016 and GPP estimates of July 11, 2016, in Shanghai, China. (a) Land cover maps from the MCD12 dataset, (b) GPP from the GPP_{VPM} dataset, and (c) GPP from the MOD17A2 dataset. Note that the MOD17A2 dataset has GPP and NPP value as zero (or Nodata) over those urban pixels that are dominated with the impervious surface.

Table 1: The impacts of urban expansion on vegetation in urban areas.

Variable	Region	Impact directions	References
Total GPP	Global	24.38–26.1 Pg C yr^{-1}	This study
GPP loss	Global	0.0061 Pg C yr^{-1}	This study
GPP	Michigan (U.S.)	Increase	Zhao et al. (2007) [52]
NPP	U.S.	Decrease	Imhoff et al. (2014); Milesi et al. (2003) [15, 57]
NPP	Global	Decrease 22.4 Tg C yr^{-1}	Liu et al. (2019) [30]
Urban vegetation growth	32 urban areas (China)	Prevalent increase	Zhao et al. (2016) [19]
Urban forest productivity	Massachusetts (U.S.)	Increase	Briber et al. (2015) [18]
Urban forest productivity	New York (U.S.)	Increase	Searle et al. (2012) [35]
Carbon stock	Denver–Boulder (U.S.)	Substantial increase	Golubiewski (2006) [58]
Carbon stock	Seattle (U.S.)	Aboveground decrease	Hutyra et al. (2011) [34]
Carbon uptake	Global	14–43 Pg C yr^{-1}	Churkina (2016) [14]
Carbon release	Global	0.05 Pg C yr^{-1}	Churkina (2016); Seto et al. (2012) [14, 10]

urbanization on vegetation cannot be focused solely on the effects of impervious surface expansion, which is only one part of urbanization. It is important to consider the effects of both UIS and UMC on vegetation in the future study of urban ecosystems.

4.3. Error Sources and Uncertainty of This Study. We recognize that urban study would be more accurate if the study area is delineated by city administrative boundary. Our global urban study is affected by (1) lack of city boundary maps for all cities in the world and (2) the difficulty to delineate the rural areas affected by urbanization as urbanization is likely to affect vegetation beyond the city boundary itself [7, 10]. Moreover, because of the mix of anthropogenic carbon emissions and vegetation carbon fluxes in urban areas, it is complex and difficult to directly observe the carbon cycle of urban area [47]. When using the grid data to define urban area, we can use satellite data such as the GOME-2 SIF data, to evaluate the GPP estimates from the models at the scale of a single grid [19, 27]. The offsetting positive and negative impacts of urbanization can help to explain the increasing trends of GPP in urban areas. The other reason is the contribution from the natural background change; global GPP also increased [38]. In terms of urban GPP, the positive effect of vegetation encompassing urban areas can offset the negative effect of UIS, and the variation of urban GPP will be partially in conformity with that of nonurban GPP.

5. Conclusions

Urbanization is complex and varies substantially over space and time, driven by varying environmental and socioeconomic

factors [59]. It is very difficult to assess the effects of urbanization on gross primary productivity of vegetation at the global scale, because we face several major issues related to the concepts, data, and methods. The major issue is the definition of urban area and the geographical domains affected by urbanization directly and indirectly. People often use city or urban administration boundary, impervious surface area, and urban system [60, 61]. In this global-scale study we used the definition of urban systems, as it allows us to study both urban sprawl and urban footprint. We used 0.5° urban gridcells, in part because we used GOME-2 SIF data at 0.5° spatial resolution to evaluate GPP data [62, 63]. In addition, we used simple linear dynamics to approximate the time course of urban expansion during 2000–2016. By using simple concept, data, and methods, this study reveals that the negative effect of urban expansion (as measured by urban impervious surface expansion) on GPP are to some degree compensated by the positive effects of urban land management, land use, local climate, and atmospheric CO_2 concentration [64–67]. This study also shows that the interannual trends of urban GPP was slightly larger than that of nonurban GPP, but the interannual variation of urban GPP was slightly smaller than that of nonurban GPP. Such analysis could be further improved in the near future after we have access to refined spatial datasets (e.g., SIF data from the TROPOMI mission and GeoCarb mission) and improved understanding of the time course of urban expansion. Our finding on the continued increases of urban GPP during 2000–2016 highlights the benefit and potential of improving urban vegetation management in the world. In the foreseeable future, more effort should be given to develop appropriate policies and management practices that could further improve urban vegetation and its management, which would help address United Nations Sustainable Development Goal #11 – Sustainable Cities and Communities.

Data Availability

The global urban area expansion dataset can be downloaded from the Seto Laboratory at Yale University (http://urban.yale.edu/data). Global gross primary (GPP) data are publicly available by doi:10.6084/m9.figshare.c.3789814. GOME-2 SIF data can be downloaded from https://avdc.gsfc.nasa.gov/pub/data/satellite/MetOp/GOME_F/.

Conflicts of Interest

The authors declare that they have no known competing financial interests or personal relationships that could have appeared to influence the work reported in this paper.

Authors' Contributions

X. X. and Y. C. designed the overall study plan. Y.C. and X.X carried out data analysis and completed the draft of this manuscript. All co-authors (J.D., Y. Z., Y. Q, R. D., X.W., X. L., J. J., and B. M. III) contributed to interpretation of the results and writing of the manuscript. J.J. provided the GOME-2 SIF data.

Acknowledgments

This work was supported in part by research grants from the US National Science Foundation (grant numbers OIA-1301789, OIA-1946093, and 1911955), the NASA Geostationary Carbon Cycle Observatory Mission (grant number 80LARC17C0001), the National Natural Science Foundation of China (grant number 42071415), and the Outstanding Youth Foundation of Henan Natural Science Foundation (grant number 202300410049). We appreciate the valuable comments provided by Karen C. Seto during the process of data analysis and manuscript writing. Urban area, GPP, and SIF data can be downloaded at http://urban.yale.edu/data, doi:10.6084/m9.figshare.c.3789814, and https://avdc.gsfc.nasa.gov/pub/data/satellite/MetOp/GOME_F/, respectively.

Supplementary Materials

Figure S1: interannual dynamics of urban and global population during 2000-2016, based on the WorldPop datasets. Figure S2: relationships between the impervious surface data of this study with that data of GLC_FCS30 in 2000 (a) and 2015 (/2016) (b) at resolution of 0.5° × 0.5°. The units of both x- and y-axis are percent (%). Figure S3: spatial distribution of correlation coefficient (r) between monthly SIF and month GPP during 2007-2016 for nonurban gridcells (a) and all the gridcells in the world (b). Figure S4: histogram of percent urban areas within individual gridcells in 2000. Figure S5: the histogram of urban expansion (% change in impervious surface within individual gridcells) between 2000 and 2016. Figure S6: the relationship between urban GPP and nonurban GPP from 2000 to 2016. *(Supplementary Materials)*

References

[1] P. Boudewyn, X. Song, S. Magnussen, and M. D. Gillis, "Global potential of biospheric carbon management for climate mitigation," *Nature Communications*, vol. 5, no. 1, pp. 1–12, 2014.

[2] X. P. Song, M. C. Hansen, S. V. Stehman et al., "Global land change from 1982 to 2016," *Nature*, vol. 560, no. 7720, pp. 639–643, 2018.

[3] K. C. Seto, B. Güneralp, and L. R. Hutyra, "Global forecasts of urban expansion to 2030 and direct impacts on biodiversity and carbon pools," *Proceedings of the National Academy of Sciences*, vol. 109, no. 40, pp. 16083–16088, 2012.

[4] J. C. Turnbull, A. Karion, K. J. Davis et al., "Synthesis of urban CO2 emission estimates from multiple methods from the Indianapolis Flux Project (INFLUX)," *Environmental Science & Technology*, vol. 53, no. 1, pp. 287–295, 2019.

[5] H. Ritchie and M. Roser, *Urbanization*, University of Oxford, United Nations, 2018.

[6] U. C. Bureau, "Urban area criteria for the 2010 census," *Federal Register*, vol. 76, pp. 53029–53043, 2011.

[7] G. Churkina, "Modeling the carbon cycle of urban systems," *Ecological Modelling*, vol. 216, no. 2, pp. 107–113, 2008.

[8] Z. Liu, C. He, Y. Zhou, and J. Wu, "How much of the world's land has been urbanized, really? A hierarchical framework

for avoiding confusion," *Landscape Ecology*, vol. 29, no. 5, pp. 763–771, 2014.

[9] O. Venter, E. W. Sanderson, A. Magrach et al., "Sixteen years of change in the global terrestrial human footprint and implications for biodiversity conservation," *Nature Communications*, vol. 7, no. 1, pp. 1–11, 2016.

[10] K. C. Seto, A. Reenberg, C. G. Boone et al., "Urban land teleconnections and sustainability," *Proceedings of the National Academy of Sciences*, vol. 109, no. 20, pp. 7687–7692, 2012.

[11] N. B. Grimm, S. H. Faeth, N. E. Golubiewski et al., "Global change and the ecology of cities," *Science*, vol. 319, no. 5864, pp. 756–760, 2008.

[12] D. E. Pataki, M. M. Carreiro, J. Cherrier et al., "Coupling biogeochemical cycles in urban environments: ecosystem services, green solutions, and misconceptions," *Frontiers in Ecology and the Environment*, vol. 9, no. 1, pp. 27–36, 2011.

[13] C. Small, C. D. Elvidge, D. Balk, and M. Montgomery, "Spatial scaling of stable night lights," *Remote Sensing of Environment*, vol. 115, no. 2, pp. 269–280, 2011.

[14] G. Churkina, "The role of urbanization in the global carbon cycle," *Frontiers in Ecology and Evolution*, vol. 3, p. 144, 2016.

[15] M. L. Imhoff, L. Bounoua, R. DeFries et al., "The consequences of urban land transformation on net primary productivity in the United States," *Remote Sensing of Environment*, vol. 89, pp. 434–443, 2004.

[16] P. Romero-Lankao, K. R. Gurney, K. C. Seto et al., "A critical knowledge pathway to low-carbon, sustainable futures: integrated understanding of urbanization, urban areas, and carbon," *Earth's Futures*, vol. 2, no. 10, pp. 515–532, 2014.

[17] Z. Ahmed, M. M. Asghar, M. N. Malik, and K. Nawaz, "Moving towards a sustainable environment: the dynamic linkage between natural resources, human capital, urbanization, economic growth, and ecological footprint in China," *Resources Policy*, vol. 67, p. 101677, 2020.

[18] B. M. Briber, L. R. Hutyra, A. B. Reinmann et al., "Tree productivity enhanced with conversion from forest to urban land covers," *PLoS One*, vol. 10, no. 8, p. e0136237, 2015.

[19] S. Zhao, S. Liu, and D. Zhou, "Prevalent vegetation growth enhancement in urban environment," *Proceedings of the National Academy of Sciences*, vol. 113, pp. 6313–6318, 2016.

[20] Q. Zhong, J. Ma, B. Zhao, X. Wang, J. Zong, and X. Xiao, "Assessing spatial-temporal dynamics of urban expansion, vegetation greenness and photosynthesis in megacity Shanghai, China during 2000-2016," *Remote Sensing of Environment*, vol. 233, p. 111374, 2019.

[21] Y. Cui, X. Xiao, Y. Zhang et al., "Temporal consistency between gross primary production and solar-induced chlorophyll fluorescence in the ten most populous megacity areas over years," *Scientific reports*, vol. 7, no. 1, pp. 1–12, 2017.

[22] A. Anav, P. Friedlingstein, C. Beer et al., "Spatiotemporal patterns of terrestrial gross primary production: a review," *Reviews of Geophysics*, vol. 53, no. 3, pp. 785–818, 2015.

[23] A. Bondeau, P. C. Smith, S. Zaehle et al., "Modelling the role of agriculture for the 20th century global terrestrial carbon balance," *Global Change Biology*, vol. 13, no. 3, pp. 679–706, 2007.

[24] S. W. Running, R. Nemani, J. M. Glassy, and P. E. Thornton, *MODIS daily photosynthesis (PSN) and annual net primary production (NPP) product (MOD17) Algorithm Theoretical Basis Document*, pp. 679–706, 1999.

[25] M. Jin, R. E. Dickinson, and D. A. Zhang, "The footprint of urban areas on global climate as characterized by MODIS," *Journal of Climate*, vol. 18, no. 10, pp. 1551–1565, 2005.

[26] D. Zhou, S. Zhao, L. Zhang, G. Sun, and Y. Liu, "The footprint of urban heat island effect in China," *Scientific Reports*, vol. 5, no. 1, p. 11160, 2015.

[27] Y. Zhang and Z. Shao, "Assessing of urban vegetation biomass in combination with LiDAR and high-resolution remote sensing images," *International Journal of Remote Sensing*, vol. 42, no. 3, pp. 964–985, 2021.

[28] X. Liu, F. Pei, Y. Wen et al., "Global urban expansion offsets climate-driven increases in terrestrial net primary productivity," *Nature communications*, vol. 10, no. 1, pp. 1–8, 2019.

[29] A. G. Aguilar, P. M. Ward, and C. B. Smith Sr., "Globalization, regional development, and mega-city expansion in Latin America: analyzing Mexico City's peri-urban hinterland," *Cities*, vol. 20, pp. 3–21, 2003.

[30] P. Martí, L. Serrano-Estrada, A. Nolasco-Cirugeda, and J. L. Baeza, "Revisiting the spatial definition of neighborhood boundaries: functional clusters versus administrative neighborhoods," *Journal of Urban Technology*, vol. 29, pp. 1–22, 2021.

[31] B. Cai and L. Zhang, "Urban CO_2 emissions in China: spatial boundary and performance comparison," *Energy Policy*, vol. 66, pp. 557–567, 2014.

[32] J. J. Walker, K. M. D. Beurs, and G. M. Henebry, "Land surface phenology along urban to rural gradients in the U.S. Great Plains," *Remote Sensing of Environment*, vol. 165, pp. 42–52, 2015.

[33] C. Bang, J. L. Sabo, and S. H. Faeth, "Reduced wind speed improves plant growth in a desert city," *PLoS One*, vol. 5, no. 6, p. pe 11061, 2010.

[34] L. R. Hutyra, B. Yoon, J. Hepinstall-Cymerman, and M. Alberti, "Carbon consequences of land cover change and expansion of urban lands: a case study in the Seattle metropolitan region," *Landscape and Urban Planning*, vol. 103, no. 1, pp. 83–93, 2011.

[35] S. Y. Searle, M. H. Turnbull, N. T. Boelman, W. S. F. Schuster, D. Yakir, and K. L. Griffin, "Urban environment of New York City promotes growth in northern red oak seedlings," *Tree Physiology*, vol. 32, no. 4, pp. 389–400, 2012.

[36] S. Bontemps, M. Boettcher, C. Brockmann et al., "Multi-year global land cover mapping at 300 M and characterization for climate modelling: Achievements of the land cover component of the ESA climate change initiative," in *In 2015 36th International Symposium on Remote Sensing of Environment*, pp. 323–328, International Society for Photogrammetry and Remote Sensing, 2015.

[37] S. Godefroid and N. Koedam, "Urban plant species patterns are highly driven by density and function of built-up areas," *Landscape ecology*, vol. 22, no. 8, pp. 1227–1239, 2007.

[38] X. Xiao, D. Hollinger, J. Aber et al., "Satellite-based modeling of gross primary production in an evergreen needleleaf forest," *Remote Sensing of Environment*, vol. 89, no. 4, pp. 519–534, 2004.

[39] Y. Zhang, X. Xiao, X. Wu et al., "A global moderate resolution dataset of gross primary production of vegetation for 2000–2016," *Scientific Data*, vol. 4, no. 1, pp. 1–13, 2017.

[40] K. Ebisu, T. R. Holford, and M. L. Bell, "Association between greenness, urbanicity, and birth weight," *Science of the Total Environment*, vol. 542, no. Part A, pp. 750–756, 2016.

[41] L. Liu, X. Zhang, Y. Gao, X. Chen, X. Shuai, and J. Mi, "Finer-Resolution mapping of global land cover: recent developments, consistency analysis, and prospects," *Journal of Remote Sensing*, vol. 2021, pp. 1–38, 2021.

[42] X. Zhang, L. Liu, X. Chen, Y. Gao, S. Xie, and J. Mi, "GLC_FCS30: Global land-cover product with fine classification system at 30 m using time-series Landsat imagery," *Earth System Science Data*, vol. 13, no. 6, pp. 2753–2776, 2021.

[43] J. Joiner, L. Guanter, R. Lindstrot et al., "Global monitoring of terrestrial chlorophyll fluorescence from moderate-spectral-resolution near-infrared satellite measurements: methodology, simulations, and application to GOME-2," *Atmospheric Measurement Techniques*, vol. 6, no. 10, pp. 2803–2823, 2013.

[44] Y. Zhang, X. Xiao, C. Jin et al., "Consistency between sun-induced chlorophyll fluorescence and gross primary production of vegetation in North America," *Remote Sensing of Environment*, vol. 183, pp. 154–169, 2016.

[45] J. Joiner, Y. Yoshida, A. P. Vasilkov et al., "The seasonal cycle of satellite chlorophyll fluorescence observations and its relationship to vegetation phenology and ecosystem atmosphere carbon exchange," *Remote Sensing of Environment*, vol. 152, pp. 375–391, 2014.

[46] Q. Weng, "Remote sensing of impervious surfaces in the urban areas: requirements, methods, and trends," *Remote Sensing of Environment*, vol. 117, pp. 34–49, 2012.

[47] X. Zhang, M. A. Friedl, C. B. Schaaf, A. H. Strahler, and A. Schneider, "The footprint of urban climates on vegetation phenology," *Geophysical Research Letters*, vol. 31, no. 12, 2004.

[48] M. Zhao, F. A. Heinsch, R. R. Nemani, and S. W. Running, "Improvements of the MODIS terrestrial gross and net primary production global data set," *Remote Sensing of Environment*, vol. 95, no. 2, pp. 164–176, 2005.

[49] M. A. White, R. R. Nemani, P. E. Thornton, and S. W. Running, "Satellite evidence of phenological differences between urbanized and rural areas of the eastern United States deciduous broadleaf forest," *Ecosystems*, vol. 5, no. 3, pp. 260–273, 2002.

[50] L. R. Hutyra, R. Duren, K. R. Gurney et al., "Urbanization and the carbon cycle: current capabilities and research outlook from the natural sciences perspective," *Earth's Futures*, vol. 2, no. 10, pp. 473–495, 2014.

[51] L. Sun, J. Chen, Q. Li, and D. Huang, "Dramatic uneven urbanization of large cities throughout the world in recent decades," *Nature Communications*, vol. 11, no. 1, pp. 1–9, 2020.

[52] T. Zhao, D. G. Brown, and K. M. Bergen, "Increasing gross primary production (GPP) in the urbanizing landscapes of southeastern Michigan," *Photogrammetric Engineering & Remote Sensing*, vol. 73, no. 10, pp. 1159–1167, 2007.

[53] S. Wu, Z. Liang, and S. Li, "Relationships between urban development level and urban vegetation states: a global perspective," *Urban Forestry & Urban Greening*, vol. 38, pp. 215–222, 2019.

[54] G. W. Luck, L. T. Smallbone, and R. O'Brien, "Socio-economics and vegetation change in urban ecosystems: patterns in space and time," *Ecosystems*, vol. 12, no. 4, pp. 604–620, 2009.

[55] S. Hussain and S. Karuppannan, "Land use/land cover changes and their impact on land surface temperature using remote sensing technique in district Khanewal, Punjab Pakistan," *Geology, Ecology, and Landscapes*, pp. 1–13, 2021.

[56] X. Tang, Y. Cui, N. Li et al., "Human Activities Enhance Radiation Forcing through Surface Albedo Associated with Vegetation in Beijing," *Remote Sensing*, vol. 12, no. 5, p. 837, 2020.

[57] C. Milesi, C. D. Elvidge, R. R. Nemani, and S. W. Running, "Assessing the impact of urban land development on net primary productivity in the southeastern United States," *Remote Sensing of Environment*, vol. 86, no. 3, pp. 401–410, 2003.

[58] N. E. Golubiewski, "Urbanization increases grassland carbon pools: Effects of landscaping in Colorado's front range," *Ecological Applications*, vol. 16, no. 2, pp. 555–571, 2006.

[59] Y. Cui, X. Xiao, R. B. Doughty et al., "The relationships between urban-rural temperature difference and vegetation in eight cities of the Great Plains," *Frontiers of Earth Science*, vol. 13, no. 2, pp. 290–302, 2019.

[60] Y. D. Wei and X. Ye, "Urbanization, urban land expansion and environmental change in China," *Stochastic Environmental Research and Risk Assessment*, vol. 28, no. 4, pp. 757–765, 2014.

[61] R. J. Pryor, "Defining the rural-urban fringe," *Social Forces*, vol. 47, no. 2, pp. 202–215, 1968.

[62] R. A. Francis, J. Lorimer, and M. Raco, "Urban ecosystems as 'natural' homes for biogeographical boundary crossings," *Transactions of the Institute of British Geographers*, vol. 37, no. 2, pp. 183–190, 2012, http://www.jstor.org/stable/41427939.

[63] L. He, J. M. Chen, J. Liu, G. Mo, and J. Joiner, "Angular normalization of GOME-2 sun-induced chlorophyll fluorescence observation as a better proxy of vegetation productivity," *Geophysical Research Letters*, vol. 44, no. 11, pp. 5691–5699, 2017.

[64] X. Lu, X. Cheng, X. Li, and J. Tang, "Opportunities and challenges of applications of satellite-derived sun-induced fluorescence at relatively high spatial resolution," *Science of the Total Environment*, vol. 619-620, pp. 649–653, 2018.

[65] J. Jiang and G. Tian, "Analysis of the impact of land use/land cover change on land surface temperature with remote sensing," *Procedia Environmental Sciences*, vol. 2, pp. 571–575, 2010.

[66] A. M. Dewan and Y. Yamaguchi, "Land use and land cover change in Greater Dhaka, Bangladesh: using remote sensing to promote sustainable urbanization," *Applied Geography*, vol. 29, no. 3, pp. 390–401, 2009.

[67] T. N. Carlson and S. T. Arthur, "The impact of land use—land cover changes due to urbanization on surface microclimate and hydrology: a satellite perspectiveGlobal and Planetary Change," vol. 25, no. 1-2, pp. 49–65, 2000.

Composition Comment

1. Please check Figures 2, 4, 6, 8, and 10 if captured correctly.